Fermi Surface reconstruction in the CDW state of $CeTe_3$ observed by photoemission

V. Brouet[1,2,3], W.L. Yang[1,2], X.J. Zhou[2], Z. Hussain[1], N. Ru[4], K.Y. Shin[4], I.R. Fisher[4] and Z.X. Shen[2,4]
[1] *Advanced Light Source, Lawrence Berkeley National Laboratory, Berkeley, CA 94720 (USA)*
[2] *Stanford Synchrotron Radiation Laboratory, Stanford university, Stanford CA 94305 (USA)*
[3] *Laboratoire de Physique des Solides, Université Paris-Sud, Bât 510, UMR 8502, 91405 Orsay (France)*
[4] *Geballe Laboratory for Advanced Materials and Department of Applied Physics, Stanford University CA 94305-4045 (USA)*
(Dated: February 6, 2008)

$CeTe_3$ is a layered compound where an incommensurate Charge Density Wave (CDW) opens a large gap ($\simeq$ 400 meV) in optimally nested regions of the Fermi Surface (FS), whereas other sections with poorer nesting remain ungapped. Through Angle-Resolved Photoemission, we identify bands backfolded according to the CDW periodicity. They define FS pockets formed by the intersection of the original FS and its CDW replica. Such pockets illustrate very directly the role of nesting in the CDW formation but they could not be detected so far in a CDW system. We address the reasons for the weak intensity of the folded bands, by comparing different foldings coexisting in $CeTe_3$.

Many electronic instabilities, such as charge and spin density waves, introduce a new periodicity in a solid, which breaks the lattice periodicity that was used to build the band structure. For a commensurate instability, it is well known that bands of the original ("extended") zone must be folded back into a smaller ("reduced") zone according to the new periodicity in order to establish the equivalency between all reduced zones. Whether this reasoning still applies to an *incommensurate* periodicity raises more complex questions [1]. Angle resolved photoemission spectroscopy (ARPES) is the most direct technique to visualize the dispersion of occupied bands and should then be an ideal witness for such behaviors. Surprisingly, the new periodicity in the CDW state is often difficult to detect, as for example in the model 2D CDW systems of $1T$-TaS_2 [2] or $2H$-$NbSe_2$ [3] families. This is mainly because the intensity of the bands folded according to the CDW periodicity, called *shadow bands*, which is proportional to the CDW coupling is often too low to be detected. The most common ARPES signature of the CDW is then the opening of a gap, either uniformly on the entire FS or solely on the FS parts presenting a good nesting. In a few cases, shadow bands have been observed *but only in the gapped regions*, as in the quasi-1D systems $(TaSe_4)_2I$ [1] or $NbSe_3$ [4].

The fate of the shadow bands in the metallic regions, when there remains some, is of fundamental interest to understand the impact of the CDW and its periodicity on the metallic properties. Many SDW/CDW systems indeed exhibit residual metallicity (as Cr [5], $NbSe_3$ [6] or $CeTe_3$ [7]) because deviation from perfect nesting leaves pockets of itinerant carriers. The reduction of the size of FS at the transition has been studied extensively [5], especially through quantum oscillations in transport or magnetic properties that are sensitive to the *area* of certain sections of the FS pockets (see for example [8] for a discussion of the situation in organic conductors). However, the location of these FS pockets, as well as their shape, could never be mapped out directly by ARPES.

We present here an ARPES study of $CeTe_3$, whose goal is precisely to reconstruct the FS of the CDW state. $CeTe_3$ is made out of square Te planes alternating with Ce/Te slabs [9]. This yields a pronounced 2D character, where the electronic properties of the magnetic slab and of the Te planes are nearly decoupled. Magnetic susceptibility measurements indicate that the Ce is trivalent [7]. The donated electrons completely fill the Te p orbitals in the Ce/Te slab and partially those in the planes [10, 11]. The metallic Te planes host an incommensurate CDW that was first detected by transmission electron microscopy (TEM) [11] and that is already present at room temperature. It is characterized by a very large gap (about 400 meV), an order of magnitude larger than in transition-metal dichalgogenides, which facilitates the study of certain aspect of the CDW. Notably, Gweon *et al.* have measured the gap anisotropy in $SmTe_3$ and shown that it can be well understood in the framework of a nesting driven CDW [12]. In this paper, we focus our attention on the modifications of a model Fermi Surface of one single Te plane, induced by the two following couplings that tend to set new periodicities.

i) *the transverse coupling between the planes and the slabs.* The 3D unit cell has a base in the (a,b) plane rotated by 45° and larger by $\sqrt{2}$ compared to the square unit of a Te plane (Fig. 2d). We will study to what extent this unit cell is relevant for describing the electronic properties of one plane.

ii) *the CDW instability.* The electron-phonon coupling stabilizes an incommensurate lattice modulation at wave vector $q_{CDW} \approx 5/7 * 2\pi/a$, where a=4.4 Å [11, 12].

In both cases, we clearly evidence the folded bands associated to these couplings and investigate further the topology of the CDW FS. Indeed, $CeTe_3$, like other RTe_3 compounds [13], remains a fairly good metal despite the large amplitude CDW, the in-plane resistivity is 50 $\mu\Omega$ cm at 300 K and the residual resistance 1 $\mu\Omega$ cm or less [7]. We show that, besides the region where the FS is destroyed by the opening of the large CDW gap, "pockets" are formed between original and folded bands.

Large single crystals of $CeTe_3$ were grown by slow cooling a binary melt [7]. The crystals cleave easily between two Te planes, providing a good surface quality for ARPES. All the data were collected at the BL 10.0.1

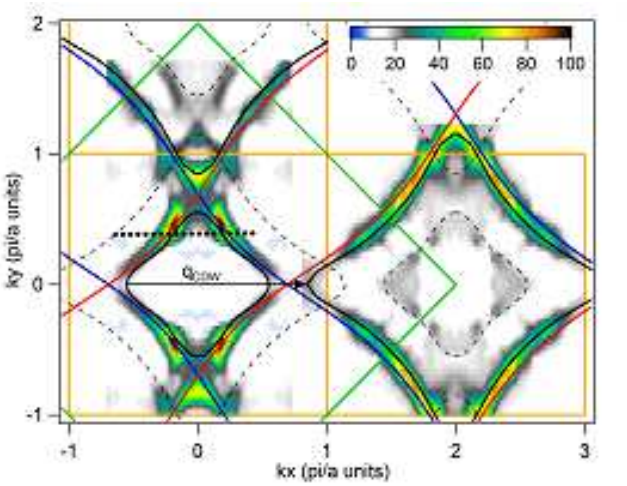

FIG. 1: Map of the spectral weight in $CeTe_3$ obtained at 25 K, with photon energy hν = 55 eV and polarization nearly perpendicular to sample surface. Orange and green lines indicate the boundaries of the reduced and extended BZ, respectively.

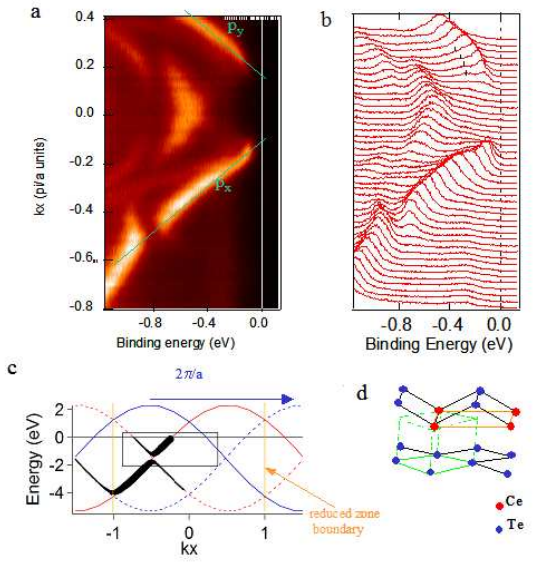

FIG. 2: (a) Color-scale image and (b) EDC stacks of the band structure for $k_y = 0.45\ \pi/a$. (c) Theoretical dispersion for p_x (solid red line), p_y (solid blue line) and the folded bands (dotted lines). The black rectangle correspond to the data shown in a. The thick black lines represent the dispersion after letting the main and folded bands interact. The thickness is proportional to the ARPES spectral weight. (d) Detail of the stacking between one Te plane and the Ce/Te slab.

of the Advanced Light Source with a Scienta SES-2002 analyser. Fig. 1 displays a map of the ARPES spectral weight in $CeTe_3$ integrated between E_F and E_F-200 meV. The main features of this map are very close from those observed in $SmTe_3$ [12], confirming the minor role of the rare earth in this electronic structure. The solid black lines are guides to the eye adjusted to the two main pieces in the map : a "square" centered at (0,0) and a larger "outer FS" part at (0,2) and (2,0). The lower intensity in the vicinity of the $k_y = 0$ axis denotes the presence of the large CDW gap in this region [12], which breaks the near equivalency between k_x and k_y. This implies that the long-range ordering of the CDW is good enough to create domains at least larger than the beam spot ($\sim$100 μm), as was also the case in previous ARPES and TEM experiments [11, 12].

A very simple electronic structure is expected for a Te plane, with perpendicular chains of p_x and p_y orbitals playing the only significant role, since band calculations show that p_z is completely filled [10, 14]. An elementary 2D tight-binding calculation including only these two orbitals, gives the following dispersion for p_x (p_y is identical but perpendicular).

$$E_{p_x}(\mathbf{k}) = t_{\parallel} \cos\left((k_x - k_y)\frac{a}{2}\right) + t_{\perp} \cos\left((k_x + k_y)\frac{a}{2}\right) \quad (1)$$

where the overlap integrals $t_{\parallel} = -4\ eV$ and $t_{\perp} = 0.75\ eV$ are taken from the calculation of Kikuchi in $LaTe_2$ [10], which contains isostructural Te planes. Fixing E_F for each orbital to contain 1.25 electrons, we obtain a contour for the FS shown as red and blue lines on Fig.1, for p_x and p_y respectively. They describe extremely well the location of the high-intensity regions in the map, except, of course, at the crossing between p_x and p_y, where their mutual interaction, totally neglected in our calculation, separates the square from the outer FS part. This good agreement leads us to use the dispersion of Eq. 1 below as a guide for backfolding the bands.

Because the system is strongly 2D, it seems natural to obtain a good description of the electronic structure with a calculation based on one Te plane. However, the stacking of the planes is such that the Brillouin Zone (BZ) in the plane for the 3D unit cell (the orange squares in Fig. 1) is different from the 2D BZ of one plane (larger green square), leading to the obvious problem that the 1st and 2nd BZ of the true 3D structure are not equivalent for the calculated FS. This equivalency should be obtained by folding back the bands along the reduced zone boundaries (or equivalently translating them by $2\pi/a$, see the sketch of Fig. 2c), which gives the dotted black contours. With data collected over many BZ (in contrast with [12]), it is clear that the intensity along this "folded FS" is drastically reduced, except near $k_y = \pm 1$ or, to a lesser extent, for the square of the second BZs. This raises questions about the meaning of the reduced or extended zone scheme for an experimental technique like ARPES. Voit *et al.* [1] recently clarified this problem by stressing that *the intensity of a folded FS in ARPES is proportional to the coupling responsible of the folding.* $CeTe_3$ clearly illustrates this principle, the lower intensity of the folded FS is a direct consequence of the weak coupling between Te planes and the magnetic slab, in other words, of the 2D character of the system [15].

The band structure along the thick dotted line of Fig. 1

is presented in Fig. 2 to detail the interactions between the main and folded bands. The two bands dispersing towards the Fermi level in Fig. 2a and 2b correspond to p_x and p_y and form the square; the bands below E_F at $k_x = 0$ probably correspond to the filled p_z orbital and will not be further discussed. Fig. 2c indicates the dispersion expected for all bands after Eq. 1. Although the folded bands are barely visible in Fig. 2a and 2b, a break in the dispersion of the main bands is clearly observed at E= - 0.8 eV, near the position expected for the crossing between the main and folded bands. Such a break typically results from the interaction between the two bands in a perturbation model. The transverse coupling $V_{3D}(q = 2\pi/a)$ opens a gap at the crossing and add a small admixture of $|k+q\rangle$ into $|k\rangle$ with a weight depending of the coupling strength and that decreases very fast away from the crossing. The new dispersion is shown by black lines in Fig. 2c with a thickness proportional to this weight, as is also the ARPES intensity [1]. This scheme also predicts that the intensity of the folded FS will be stronger near the zone boundary at $k_y = \pm 1$, because the bands cross there nearer to E_F, as is observed.

Let us note that, although there are two Te planes per unit cell, shifted by a/2 with respect to each other, this stacking does not define a new unit cell and, therefore, does not induce any folding. On the other hand, it could split p_x and p_y into two bands, similarly to the bilayer splitting well-known from ARPES studies of $Bi_2Sr_2CaCu_2O_{8+\delta}$ [16]. This could be the origin of the shoulder of p_y indicated by black dots in Fig. 2b. The intensity of this shoulder strongly depends on photon energy, it is nearly as intense as the main band at 35 eV.

We have discussed this folding in some details, because the formation of the CDW can be described in identical terms, only the origin of the coupling is different and the periodicity is incommensurate. A spontaneous distortion of the lattice at wave vector q will be stabilized if this allows enough pairs of states $|k\rangle$ and $|k+q\rangle$ to lower their energies through the opening of a gap at E_F. This is the case here for q_{CDW}, which nests the square into the outer FS part (see Fig. 1). For clarity, we will refer in the following to the bands induced by the 3D structure as "folded bands" and to those of the CDW as "shadow bands". We can anticipate to observe weak shadow bands at position translated by q_{CDW} from the main bands that will :
i) either interact with the main band to create the CDW gap, if they cross near E_F (more precisely, if the distance between the crossing and E_F is smaller than the gap).
ii) or draw a FS replica that closes the FS pockets, when the bands cross away from E_F, i.e. for poorer nesting.

Fig. 2b gives an example of the first case, that of the gap formation. It shows that p_x and p_y clearly *bend away* from E_F, leaving a gap $\Delta \simeq 120$ meV (at this position, the gap has significantly reduced). This bending is due to the connection with the CDW shadow band, exactly as in the case previously studied, but with an upper branch, above E_F, that cannot be observed.

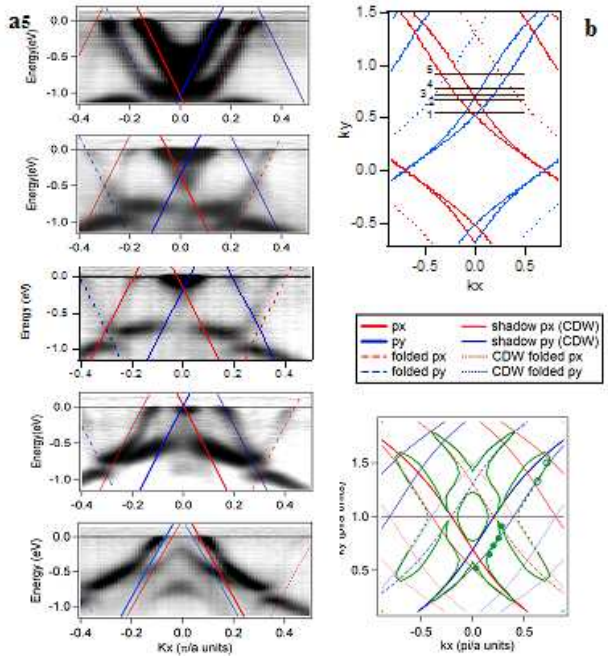

FIG. 3: a1 to a5: Band structure for k_y=0.6, 0.69, 0.73, 0.77 and 0.91. A background was substracted and the gray scale is logarithmic. The lines represent dispersion from Eq.1 and backfolded bands (see legend). b) Location of the cuts of part a in the reciprocal space with theoretical traces of the main, folded and shadow FS. c) Sketch of the FS pockets reconstructed from the different FS traces (green lines, the dashed part is not observed experimentally). The green points locate the observed E_F crossings on the shadow FS (solid symbols correspond to images of part a).

The second case, that of FS pockets, occurs in the metallic region and is detailed in the images of Fig. 3. In the bottom image a1, at $k_y = 0.6$, the hole-like square has become ungapped and is nearly closing. For higher k_y values, the electron-like outer FS piece of FS develops itself around $k_x = 0$. This evolution follows very well the theoretical dispersion of Eq. 1, shown as thick blue and red lines. In this region, the folded outer FS is also quite clear, giving rise to a second parabola, which becomes increasingly visible from a1 to a5 (dotted lines). However, two other weak lines are visible, most clearly in image a3. They cannot be attributed to a substructure of another line, such as the bilayer splitting previously discussed, because their slope is opposite to that of the next dotted or thick lines [14]. *They are the CDW shadow bands*, their position exactly matches the one of p_x or p_y translated by q_{CDW} (thin blue or red line) and so does their evolution as a function of k_y. The location of the different cuts are indicated in Fig. 3b and the Fermi level crossings on the shadow part of the FS are reported by green points on Fig. 3c. When approaching the square, the continuity strongly suggests that the shadow FS smoothly connects to the original square and that the two bands joining each other just below E_F in

image a1 (green dots) actually correspond to the closed CDW replica. However, bilayer splitting effects become harder to rule out after the shadow and main bands have crossed and appear parallel.

By connecting the green points, we may start to draw the green line in Fig. 3c indicating the contour of the new FS. To complete this contour, we use the intersection of the main, folded and shadow FS as a guide. This suggests two different pockets. The first one, the oval centered at (0,1), is electron-like and is formed by the interaction between the direct and folded FS. The second pocket is hole-like and extends from the top of the square to the outer FS branches. We have discussed its lower part with Fig. 3a. Along most part of the outer FS (shown by dashed green line in Fig. 3c), we do not detect shadow bands, although we clearly see a break in the dispersion where we expect their crossing (just like for the folded bands in Fig. 2). This lower intensity is expected theoretically because the nesting is the worst there. At the very end of the pocket, we observe shadow bands again at positions indicated by open green circles. This allows to pursue the solid green line around the closure of the pockets on the outer FS part.

The determination of this green contour was the main purpose of this paper, as it defines the shape of the metallic pockets. However, it is only a first approximation of the FS, because we have restricted our study to the first shadow bands. For the incommensurate CDW, multiple of q_{CDW} should create an infinity of new bands. The weight of these higher order shadow bands decreases very fast, which not only means that they will not be observable experimentally, but also that their role for many properties (e.g. transport) will become negligible. Because of this, the absence of true periodicity introduced by the incommensurate CDW does not destroy the electronic structure, a situation comparable to that of quasicrystals [17]. Similarly, the spectral weight changes along the green contour, so that the quasi-classical description of electronic orbits become non-trivial. However, for each pair of $|k\rangle$ and $|k+q\rangle$ on the "two sides" of the pocket, there will be another pair at $|k'=k+q\rangle$ and $|k'-q\rangle$ with opposite weights, so that the symmetry is maintained. Each quasiparticles of wave vector k acquires some component at vector k$\pm$q and interferences between them can occur. Recently, we have observed quantum oscillations in the magnetization of $LaTe_3$ [7], which is a promising step towards a very complete determination of the RTe_3 FS. For fields oriented perpendicular to the Te planes, we observe osciallations at approximate frequencies 0.5 and 1.6kT and the former probably corresponds to the small oval pocket centered at (0,1).

To summarize, $CeTe_3$ is particularly well suited for a detailed study of FS topology in presence of an incommensurate periodicity. The simplicity of the electronic structure of the Te planes makes it an ideal ground to test the impact of perturbations. ARPES for example offers a simple image of the way the 2D electronic structure is modified by the 3D couplings. It also clearly locates the CDW gap on the best nested parts of the original FS and further reveals new bands closing the FS that can be directly traced back to the CDW periodicity. This supports intimately the description of the CDW as a nesting driven FS instability, whereas, because of the large gap, it was a priori not obvious that the CDW could still be viewed as a perturbation of the metallic state. One could rather have started from a localized picture, where the tendency of Te to form dimers with its neighbors would be the driving force of a structural distortion. Our study clarifies the original metallic properties arising from this situation, characterized by strong in-plane and out-of-plane anisotropy. As a result, the FS first appears as made of *arcs* that are not reaching the zone boundaries. This situation is reminiscent of that of complex materials exhibiting pseudogaps in some directions, as in certain phases of cuprates [16]. In $CeTe_3$, we demonstrate, for the first time in a CDW material, that these arcs can be explained to a very good approximation as in fact formed of narrow pockets resulting from the interaction between the original FS and its CDW replica.

The SSRL's effort is supported by DOE's Office of Basic Energy Sciences, Division of Materials Science with contract DE-FG03-01ER45929-A001. The work at Stanford was supported by ONR grant N00014-98-1-0195-P0007 and NSF grant DMR-0304981.

[1] J. Voit *et al.*, Science **290**, 501 (2000)
[2] Th. Pillo *et al.*, Phys. Rev. B **64**, 245105 (2001)
[3] Th. Straub *et al.*, Phys. Rev. Lett. **82**, 4504 (1999)
[4] J. Schafer *et al.*, Phys. Rev. Lett. **87**, 196403 (2001)
[5] E. Fawcett, Rev. of Modern Phys. **60**, 209 (1988)
[6] N.P. Ong and P. Monceau, Phys. Rev. B **16**, 3443 (1977)
[7] N. Ru, I.R. Fisher *et al.*, in preparation
[8] X. Yan *et al.*, Phys. Rev. B **36**, 1799 (1987); S. Uji *et al.*, Phys. Rev. B **53**, 14399 (1996); A. Audouard *et al.*, Phys. Rev. B **50**, 12726 (1994)
[9] B.K. Norling and H. Steinfik, Inorganic Chemistry, **5**, 1488 (1966)
[10] A. Kikuchi, J. of the Phys. Soc. of Japan **67**, 1308 (1998)
[11] E. DiMasi *et al.*, Phys. Rev. B **52**, 14516 (1995). Compared to this paper, we use the equivalent (1-q_{CDW}) to make the nesting of the FS more apparent on Fig. 1.
[12] G.H. Gweon *et al.*, Phys. Rev. Lett. **81**, 886 (1998)
[13] E. DiMasi, B. Foran, M.C. Aronson and S. Lee, Chem. Mater. **6**, 1867 (1994)
[14] S. Dugdale *et al.*, to be published. Calculations predict a parallel bilayer splitting of at most 0.05 π/a.
[15] With photon energies from 25 to 55 eV and different polarizations, the relative weight of p_x and p_y changes significantly but the folded FS is always significantly weaker.

[16] A. Damascelli, Z. Hussain and Z.-X. Shen, Rev. of Modern Physics **75**, 473 (2003)
[17] F. Piéchon, M. Benakli and A. Jagannathan, Phys. Rev. Lett. **74**, 5248 (1995)